High Multiplicity pp and pA: explosive Stringy Pomeron and Hydrodynamics at its Edge

arXiv:1301.4470

Edward Shuryak and Ismail Zahed

Stony Brook

Talk at RBRC workshop, April 2013

2 parts:

micro=>macro

macro=>micro

micro-to-macro:
excitation of stringy Pomeron

- stringy Pomeron: Stoffers-Zahed model
- T=>T(Hagedorn) in bulk and for one string
- transition to explosive regime
- black hole connection

stringy Pomeron

A. Stoffers and I. Zahed, arXiv:1211.3077 [nucl-th].
I. Zahed, arXiv:1211.6421 [hep-ph].

At very high energies the rapidity interval parameter is large

$$\chi = \ln(s/s_0) \gg 1 \tag{48}$$

and will play the role of the *effective time* in

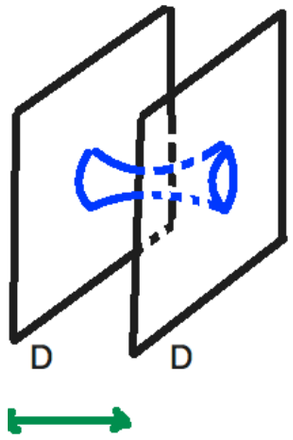

sion. Two longitudinal directions – time and the beam direction, also often used as light cone variables $x_\pm$ – are complemented by two transverse coordinates plus a *"scale coordinate"* z. Its initial value corresponds to a physical size of the colliding dipoles and diffusion means the production of small size closed strings. The z-coordinate is not flat. We will model its metric by an AdS_5 with a wall. The number of transverse coordinates, which will play an important role in the following, is thus

$$D_\perp = 3 \tag{49}$$

$$\frac{1}{-2is}\mathcal{T}(s,t;k) \approx g_s^2 \int d^2\mathbf{b}\, e^{iq\cdot\mathbf{b}}\, \mathbf{K}_T(\beta,\mathbf{b};k) \tag{50}$$

where $\mathbf{K}_T$ is the pomeron propagator for dipole sources of color N_c-ality k describing the string flux. k runs over all integers till $N_c/2$ for even N_c and $N_c/2+1/2$ for odd ones. In the real world with the SU(3) color group, $k=1$ is the usual string between fundamental charges (quarks) and the largest tension $k=2$ is the one between two baryon junctions. The first argu-

$$\mathcal{T}(s,t;k) \approx i g_s^2 \left(\frac{s}{s_0}\right)^{1+\frac{kD_\perp}{12}+\frac{\alpha'}{2k}t} \tag{59}$$

Thus the resulting pomeron is supercritical, with the intercept above 1

$$\alpha_{\mathbf{P},k}(0) = 1 + \frac{kD_\perp}{12} \to 1 + \frac{kD_\perp}{12} - \frac{(D_\perp-1)^2}{8\sqrt{\lambda}} \tag{60}$$

where the first term is due to Casimir-Luscher contribution and the $1/\sqrt{\lambda}$ correction follows from the tachyonic correction (58) as discussed in [1].

$D_k\chi$. A more precise bound follows from the inclusion of the $1/\lambda$ corrections in the tachyon mass (58) or

$$\beta > \sqrt{2(\alpha_{\mathbf{P}}-1)}\,\beta_H \tag{61}$$

This leads to the bound $\chi < 10$ for the corrected phenomenological value of the pomeron intercept $\alpha_{\mathbf{P}} - 1 = 0.08$ in (60), which roughly corresponds to energies below the LHC. This

now our paper

a stringy cylinder generates temperature, entropy and even viscosity (Kubo)

1/T is circle's sircumference,

so T is highest at the middle

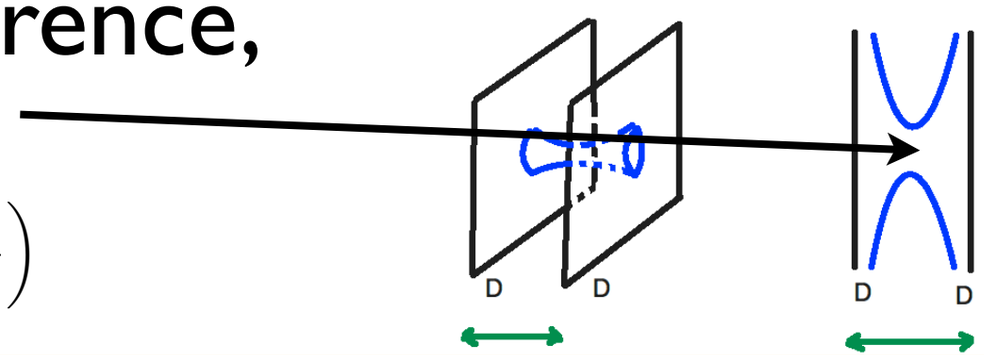

$$\mathbf{S} = -D_\perp \sum_{n=1}^{\infty} \left(\ln\left(1 - e^{-\beta_k n}\right) + \frac{\beta_k n}{e^{\beta_k n} - 1} \right)$$
$$+D_\perp \left(\frac{\beta_k}{12} - \frac{1}{2}\left(1 + \ln\left(\frac{\beta_k}{2\pi}\right)\right)\right)$$

Pure glue thermodynamics

Near-Hagedorn regime: a string gets excited into a **string ball,** with growing **entropy,energy** but **not free energy (=p)!**

a b

Polyakov, Susskind 1978

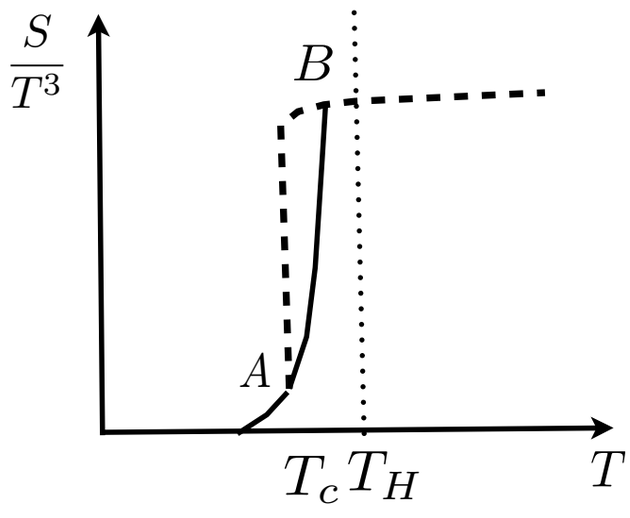

FIG. 2: Schematic temperature dependence of the entropy density. The dashed line represents equilibrium gluodynamics with a first order transition at $T = T_c$. The solid line between points A and B represents the expected behavior of a single string approaching its Hagedorn temperature T_H.

but when T is too close to T(Hagedorn), transition to QGP happens, pressure grows and the ball can explode!

T=>T_H

Hagedorn regime
string makes a ball
small F,p
large E,S

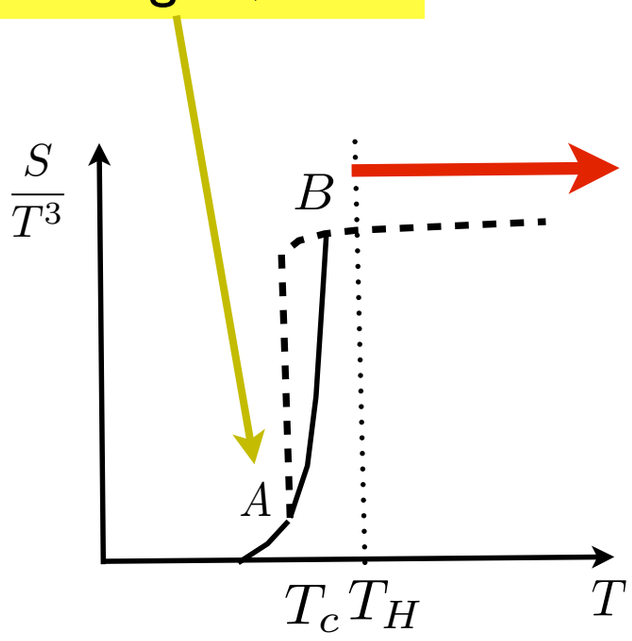

FIG. 2: Schematic temperature dependence of the entropy density. The dashed line represents equilibrium gluodynamics with a first order transition at $T = T_c$. The solid line between points A and B represents the expected behavior of a single string approaching its Hagedorn temperature T_H.

$$\frac{\Delta\beta}{\beta_H} = \frac{T_H}{T} - 1 = \mathcal{O}\left(\frac{1}{N_c}\right)$$

The ratio of the high multiplicity events to the minimum bias events can be estimated as

$$\frac{\sigma_{HM}}{\sigma_{MB}} \approx g_s^2 \frac{1}{\chi^{D_\perp/2}} \left(\frac{\Delta\beta}{\beta_H}\right) e^{-\chi\sqrt{\Delta\beta/2\beta_H}} \quad (72)$$

where we have dropped an overall number of order 1 and $D_\perp = 3$. For near critical strings we have (70) and $g_s \approx 1/N_c$. At LHC, $\chi \approx 10$ so that

$$\frac{\sigma_{HM}}{\sigma_{MB}} \approx 10^{-5} \quad (73)$$

This estimate is comparable to the probability of the high multiplicity trigger used by the CMS collaboration for events displaying the ridge in pp collisions at LHC.

a string ball is dual to a black hole

The correspondence is usually derived via the entropy

(=Hawking-Bekenstein)

But one can also calculate viscosity, which gives 1/4pi

although the calculation is stringy not BH. (And even if BH it is very different from that in AdS/CFT , not located in 5-th dimension, so were surprised)

Kubo

tensor. To assess the primordial viscosity, we follow [2] and write the needed expression on the streched horizon for the excited string

$$\eta_R = \lim_{\omega_R \to 0} \frac{A_R}{2\omega_R} \int_0^\infty d\tau e^{i\omega_R \tau} \mathbf{R}_{23,23}(\tau) \quad (87)$$

with A_R the area of the black-hole and τ a dimensionless Rindler time. The retarded commutator of the normal ordered transverse stress tensor for the Polyakov string on the Rindler horizon reads

$$\mathbf{R}_{23,23}(\tau) = \left\langle \left[T_\perp^{23}(\tau), T_\perp^{23}(0) \right] \right\rangle \quad (88)$$

with

$$T_\perp^{23}(\tau) = \frac{1}{2A_R} \sum_{n \neq 0} : a_n^2 a_n^3 : \, e^{-2in\tau} \quad (89)$$

and the canonical rules $\left[a_m^i, a_n^j\right] = m\delta_{m+n,0}\delta^{ij}$. The averaging in (88) is carried using the black-body spectrum as in (84). The result is

$$\eta_R = \lim_{\omega_R \to 0} \frac{A_R}{2\omega_R} \frac{\pi}{2A_R^2} \frac{(\omega_R/2)^2}{e^{\beta_R \omega_R/2} - 1} = \frac{1}{A_R} \frac{\pi}{8\beta_R} \quad (90)$$

We note the occurence of the Bekenstein-Hawking or Rindler temperature $\beta_{BH} = \beta_R$ in the thermal factor.

Combining (86) for the entropy to (90) yields the viscosity on the streched horizon

$$\frac{\eta_R}{\mathbf{S_R}/A_R} = \frac{1}{4\pi} \left(\frac{3}{D_\perp} \right) \equiv \frac{1}{4\pi} \quad (91)$$

summary
micro=>macro

- at very high energy the strings of the Pomeron gets longer and effectively hotter
- as its T approach Haderon temperature, a string ball regime appears => high S,E but not p
- as T grows too close to T(Hagedorn), string ball saturates the space and transition to sQGP happens. => p grows =>hydro explosion

Macro to micro: Outline

Macro to micro: Outline

- history before LHC

Macro to micro: Outline

- history before LHC
- 4 papers from LHC experiments

Macro to micro: Outline

- history before LHC
- 4 papers from LHC experiments
- two small parameters of hydro

Macro to micro: Outline

- history before LHC
- 4 papers from LHC experiments
- two small parameters of hydro
- the radial flow, gradients and viscosity

Macro to micro: Outline

- history before LHC
- 4 papers from LHC experiments
- two small parameters of hydro
- the radial flow, gradients and viscosity
- higher harmonics, sound damping

Macro to micro: Outline

- history before LHC
- 4 papers from LHC experiments
- two small parameters of hydro
- the radial flow, gradients and viscosity
- higher harmonics, sound damping
- higher harmonics for pp and pA

Macro to micro: Outline

- history before LHC
- 4 papers from LHC experiments
- two small parameters of hydro
- the radial flow, gradients and viscosity
- higher harmonics, sound damping
- higher harmonics for pp and pA
- higher gradients and LS resummation

prehistory:

Can there be hydro in pp?

prehistory:

Can there be hydro in pp?

- **the radial flow should affect pi,K,p differently** => but pp ISR data showed no effect (excellent Mt scaling)

E. V. Shuryak and O. V. Zhirov, Phys. Lett. B 89, 253 (1979).

prehistory:

Can there be hydro in pp?

- **the radial flow should affect pi,K,p differently** => but pp ISR data showed no effect (excellent Mt scaling)

  E. V. Shuryak and O. V. Zhirov, Phys. Lett. B 89, 253 (1979).

- 20 years later Bjorken and co [MiniMax Collaboration], T. C. Brooks et al. Phys. Rev. D 61, 032003 (2000) [hep-ex/9906026] took data at TEVATRON: minor effect, inconclusive

prehistory:

Can there be hydro in pp?

- **the radial flow should affect pi,K,p differently** => but pp ISR data showed no effect (excellent Mt scaling)

  E. V. Shuryak and O. V. Zhirov, Phys. Lett. B 89, 253 (1979).

- 20 years later Bjorken and co [MiniMax Collaboration], T. C. Brooks et al. Phys. Rev. D 61, 032003 (2000) [hep-ex/9906026] took data at TEVATRON: minor effect, inconclusive

- the radial flow was seen in AA at AGS/SPS
  Good pre-RHIC hydro description C.Hung,E.Shuryak Phys.Rev. C57 (1998) 1891-1906

prehistory:

Can there be hydro in pp?

- **the radial flow should affect pi,K,p differently** => but pp ISR data showed no effect (excellent Mt scaling)

  E. V. Shuryak and O. V. Zhirov, Phys. Lett. B 89, 253 (1979).

- 20 years later Bjorken and co [MiniMax Collaboration], T. C. Brooks et al. Phys. Rev. D 61, 032003 (2000) [hep-ex/9906026] took data at TEVATRON: minor effect, inconclusive

- the radial flow was seen in AA at AGS/SPS
  Good pre-RHIC hydro description C.Hung,E.Shuryak Phys.Rev. C57 (1998) 1891-1906

- and everyone knows what happened at RHIC, v_n etc

LHC era begins

Observation of long-range, near-side angular correlations in pPb collisions at the LHC

The CMS Collaboration*

high multiplicity trigger in pp reveals a ``ridge"
which is also there in pPb

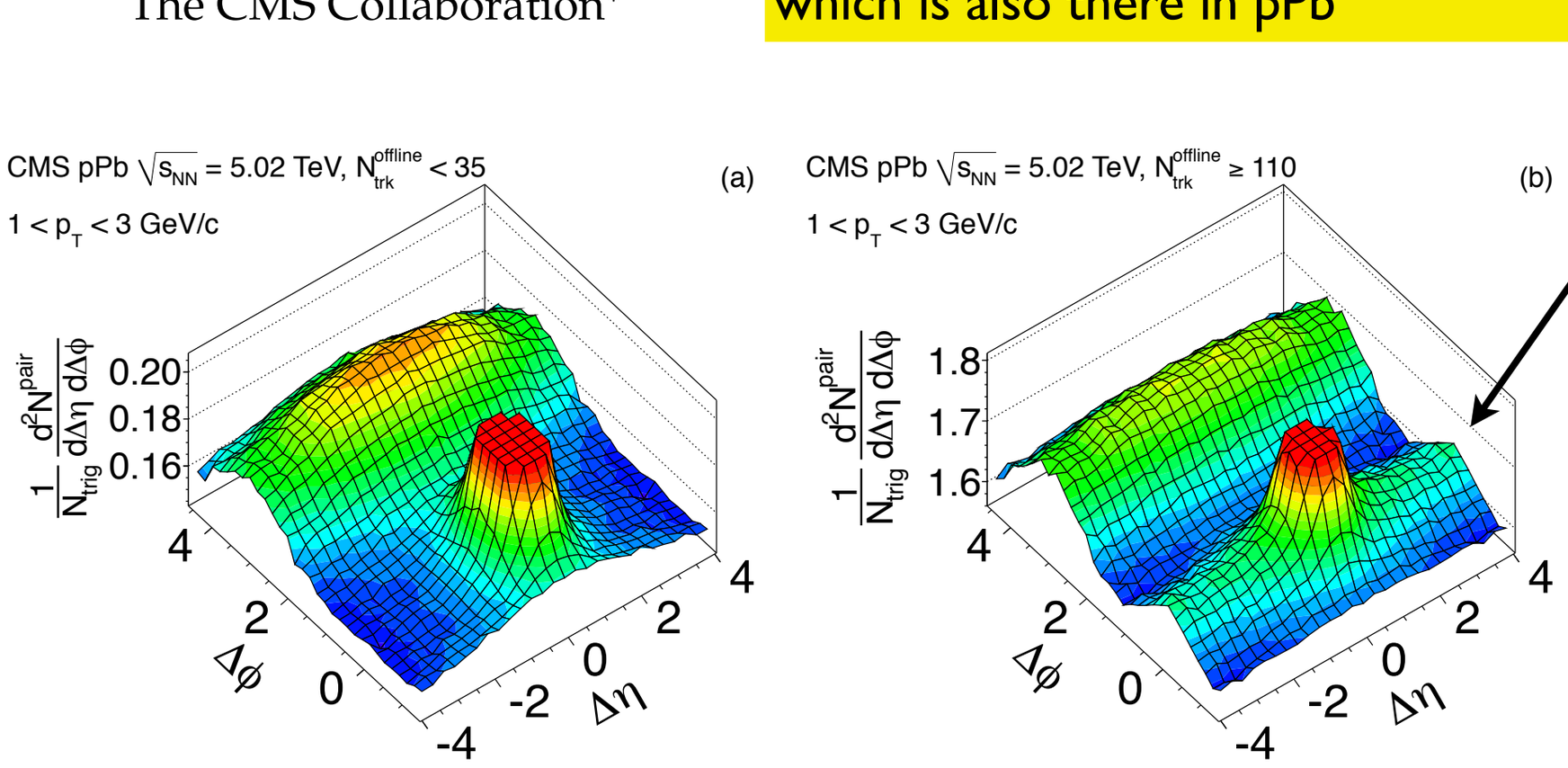

Figure 1: 2-D two-particle correlation functions for 5.02 TeV pPb collisions for pairs of charged particles with $1 < p_{\mathrm{T}} < 3\,\mathrm{GeV}/c$. Results are shown (a) for low-multiplicity events ($N_{\mathrm{trk}}^{\mathrm{offline}} < 35$) and (b) for a high-multiplicity selection ($N_{\mathrm{trk}}^{\mathrm{offline}} \geq 110$). The sharp near-side peaks from jet correlations have been truncated to better illustrate the structure outside that region.

- all bins show back-to-back correlation well described by ``minijet'' models like HIJING
- Ridge is a peak at the same azimuth, seen at highest multiplicity only and at pr=1-2 GeV
- it is stronger in pA than at pp, yet the same multiplicity is needed

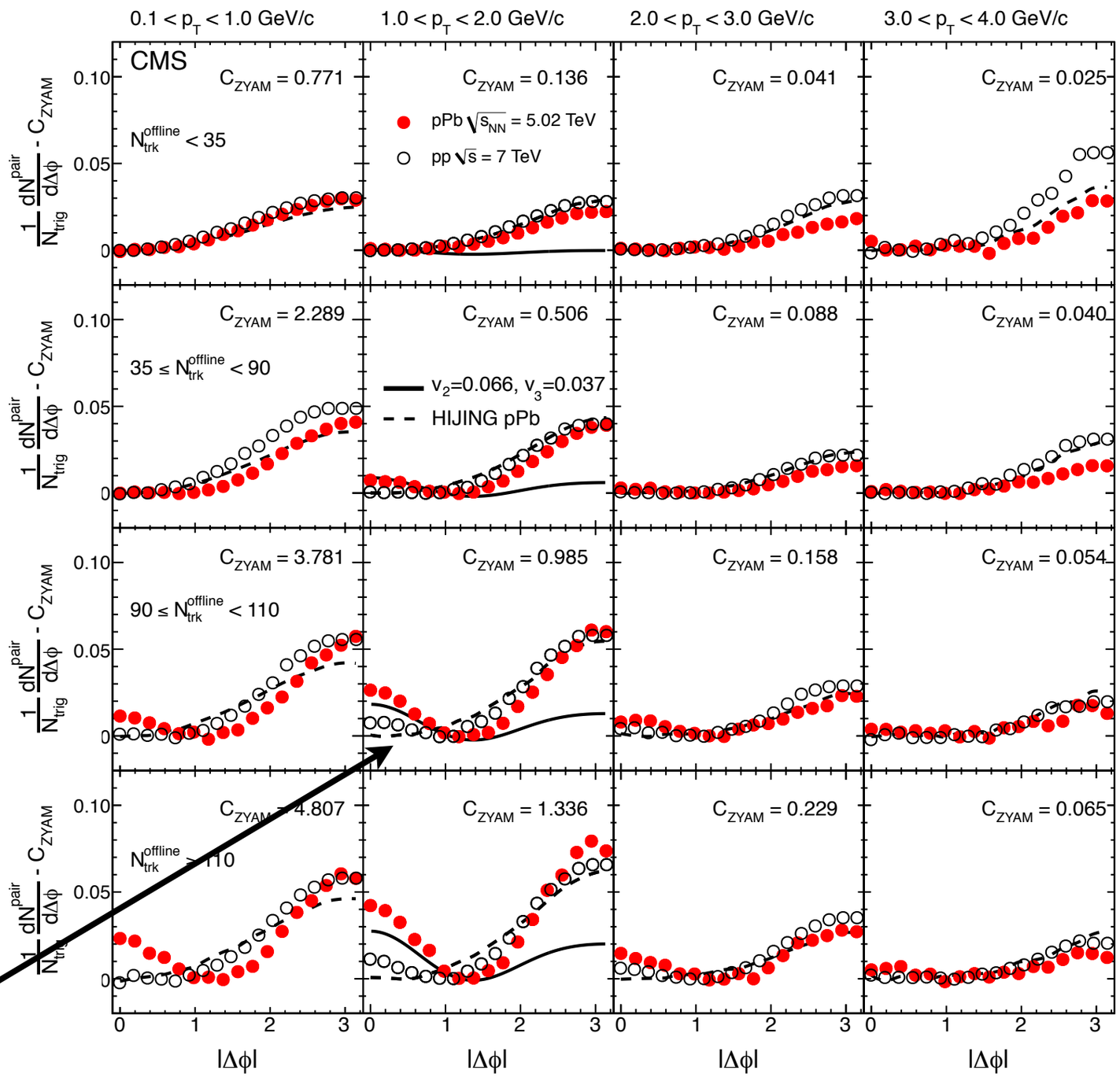

Figure 2: Correlated yield obtained from the ZYAM procedure as a function of $|\Delta\phi|$ averaged over $2 < |\Delta\eta| < 4$ in different p_{T} and multiplicity bins for 5.02 TeV pPb data (solid circles) and 7 TeV pp data (open circles). The p_{T} selection applies to both particles in each pair. Statistical uncertainties are smaller than the marker size. The subtracted ZYAM constant is listed in each panel. Also shown are pPb predictions for HIJING [24] (dashed curves) and a hydrodynamic model [25] (solid curves shown for $1 < p_{\mathrm{T}} < 2\,\mathrm{GeV}/c$).

- a ``double ridge'' in ALICE and ATLAS

Long-range angular correlations on the near and away side in p–Pb collisions at $\sqrt{s_{NN}}$= 5.02 TeV

ALICE Collaboration*

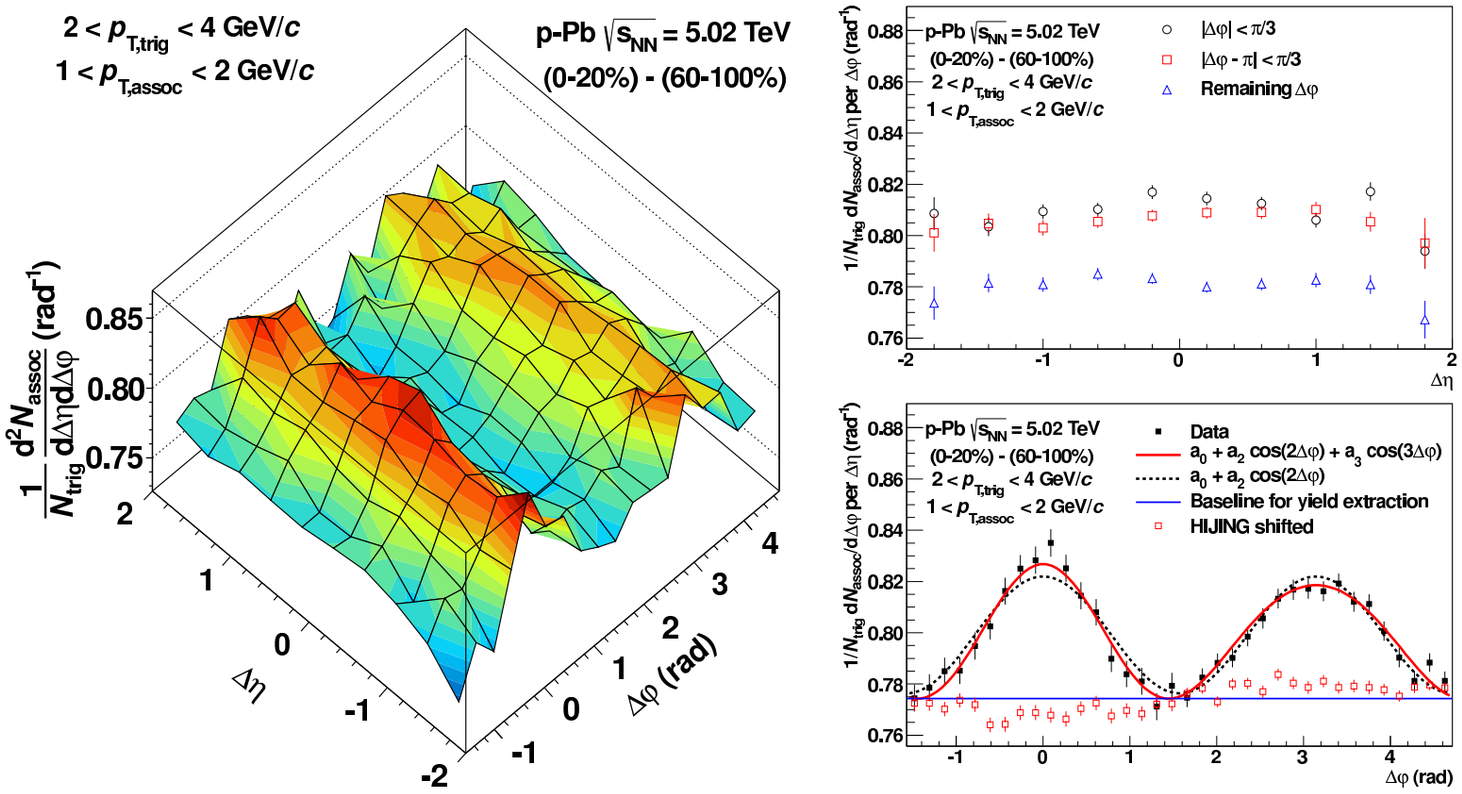

Fig. 3: Left: Associated yield per trigger particle in $\Delta\varphi$ and $\Delta\eta$ for pairs of charged particles with $2 < p_{\mathrm{T,trig}} < 4$ GeV/c and $1 < p_{\mathrm{T,assoc}} < 2$ GeV/c in p–Pb collisions at $\sqrt{s_{\mathrm{NN}}} = 5.02$ TeV for the 0–20% multiplicity class, after subtraction of the associated yield obtained in the 60–100% event class. Top right: the associated per-trigger yield after subtraction (as shown on the left) projected onto $\Delta\eta$ averaged over $|\Delta\varphi| < \pi/3$ (black circles), $|\Delta\varphi - \pi| < \pi/3$ (red squares), and the remaining area (blue triangles, $\Delta\varphi < -\pi/3$, $\pi/3 < \Delta\varphi < 2\pi/3$ and $\Delta\varphi > 4\pi/3$). Bottom right: as above but projected onto $\Delta\varphi$ averaged over $0.8 < |\Delta\eta| < 1.8$ on the near side and $|\Delta\eta| < 1.8$ on the away side. Superimposed are fits containing a $\cos(2\Delta\varphi)$ shape alone (black dashed line) and a combination of $\cos(2\Delta\varphi)$ and $\cos(3\Delta\varphi)$ shapes (red solid line). The blue horizontal line shows the baseline obtained from the latter fit which is used for the yield calculation. Also shown for comparison is the subtracted associated yield when the same procedure is applied on HIJING shifted to the same baseline. The figure shows only statisti-

• a ``double ridge" in ALICE and ATLAS

Long-range angular correlations on the near and away side in p–Pb collisions at $\sqrt{s_{NN}}$= 5.02 TeV

ALICE Collaboration*

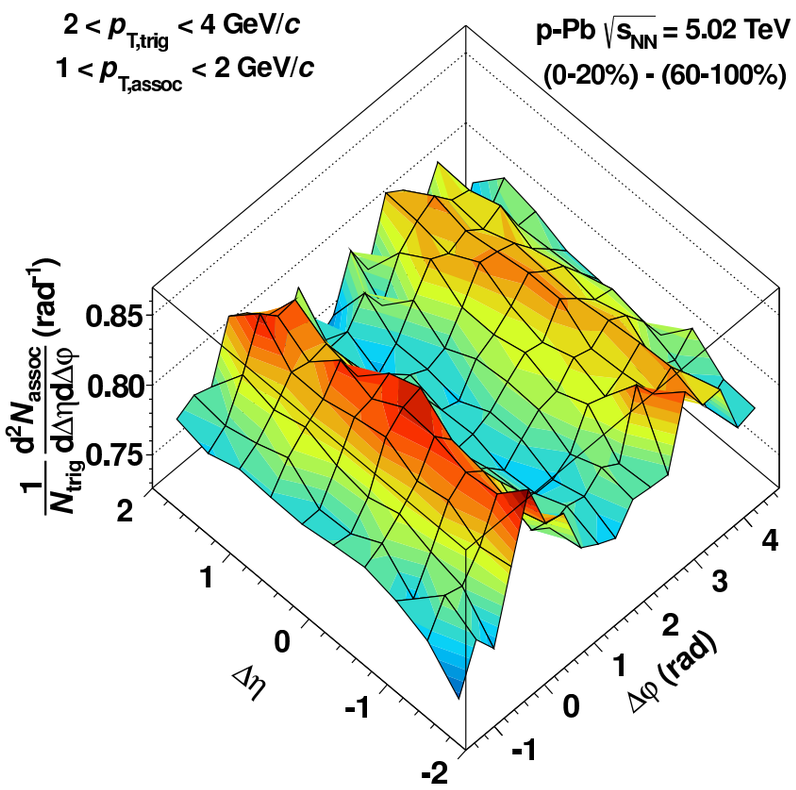

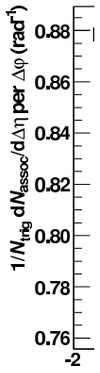

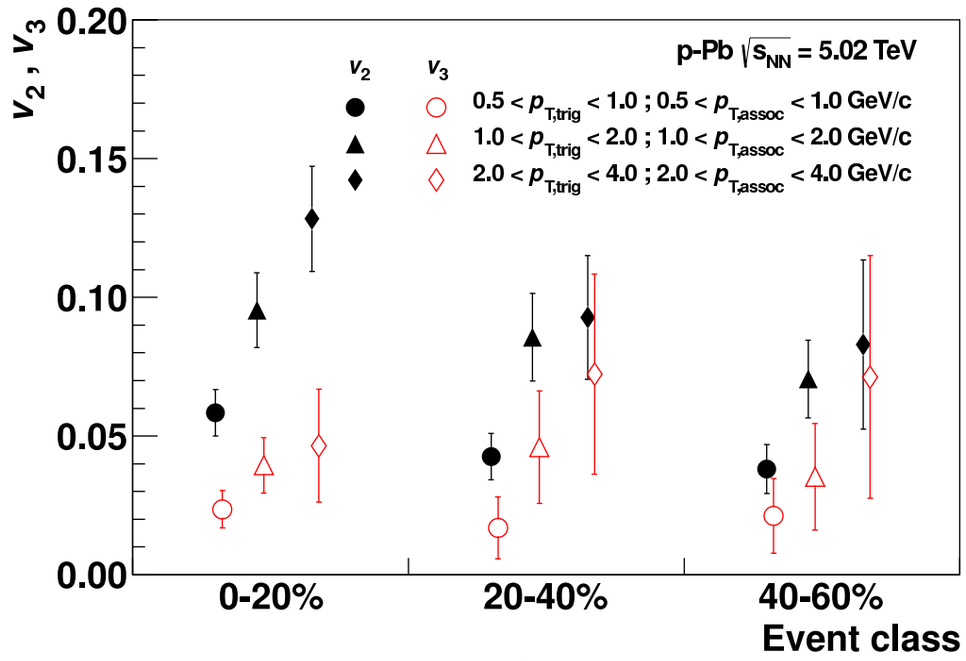

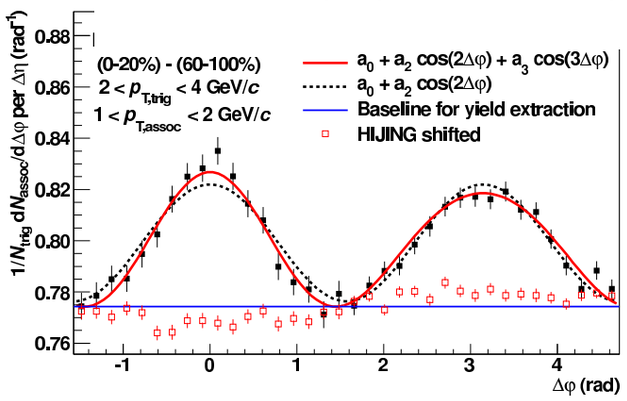

Fig. 3: Left: Associated yield per trigger particle in $\Delta\varphi$ and $\Delta\eta$ for pairs of charged particles with $2 < p_{\mathrm{T,trig}} < 4$ GeV/c and $1 < p_{\mathrm{T,assoc}} < 2$ GeV/c in p–Pb collisions at $\sqrt{s_{\mathrm{NN}}} = 5.02$ TeV for the 0–20% multiplicity class, after subtraction of the associated yield obtained in the 60–100% event class. Top right: the associated per-trigger yield after subtraction (as shown on the left) projected onto $\Delta\eta$ averaged over $|\Delta\varphi| < \pi/3$ (black circles), $|\Delta\varphi - \pi| < \pi/3$ (red squares), and the remaining area (blue triangles, $\Delta\varphi < -\pi/3$, $\pi/3 < \Delta\varphi < 2\pi/3$ and $\Delta\varphi > 4\pi/3$). Bottom right: as above but projected onto $\Delta\varphi$ averaged over $0.8 < |\Delta\eta| < 1.8$ on the near side and $|\Delta\eta| < 1.8$ on the away side. Superimposed are fits containing a $\cos(2\Delta\varphi)$ shape alone (black dashed line) and a combination of $\cos(2\Delta\varphi)$ and $\cos(3\Delta\varphi)$ shapes (red solid line). The blue horizontal line shows the baseline obtained from the latter fit which is used for the yield calculation. Also shown for comparison is the subtracted associated yield when the same procedure is applied on HIJING shifted to the same baseline. The figure shows only statisti-

• a ``double ridge" in ALICE and ATLAS

Long-range angular correlations on the near and away side in p–Pb collisions at $\sqrt{s_{NN}}$= 5.02 TeV

ALICE Collaboration*

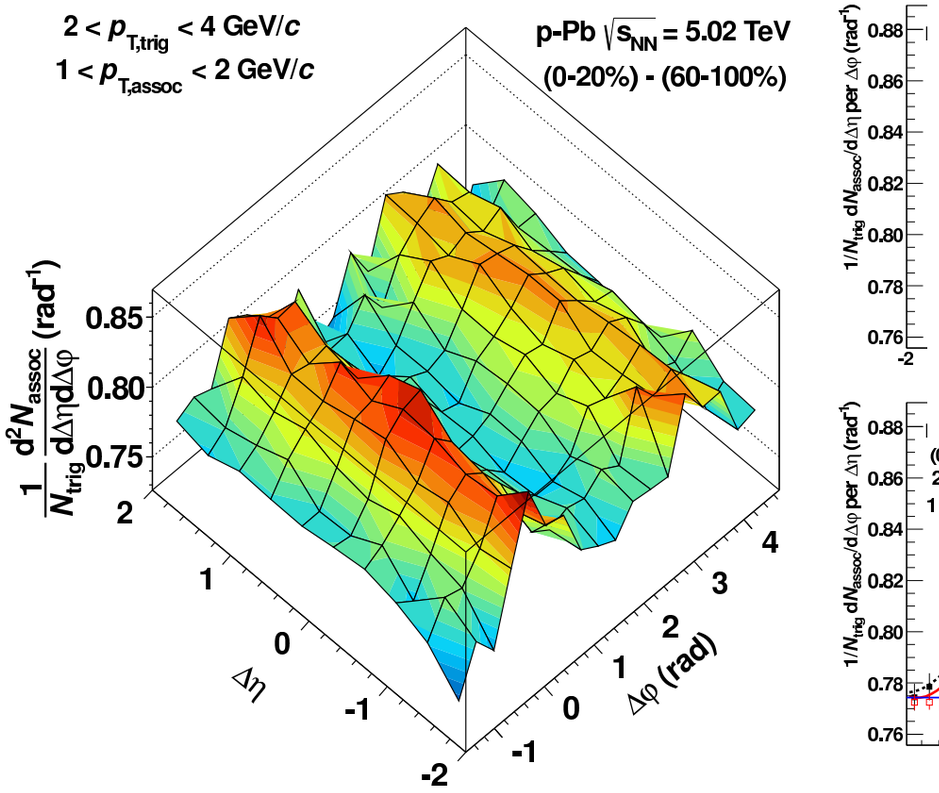

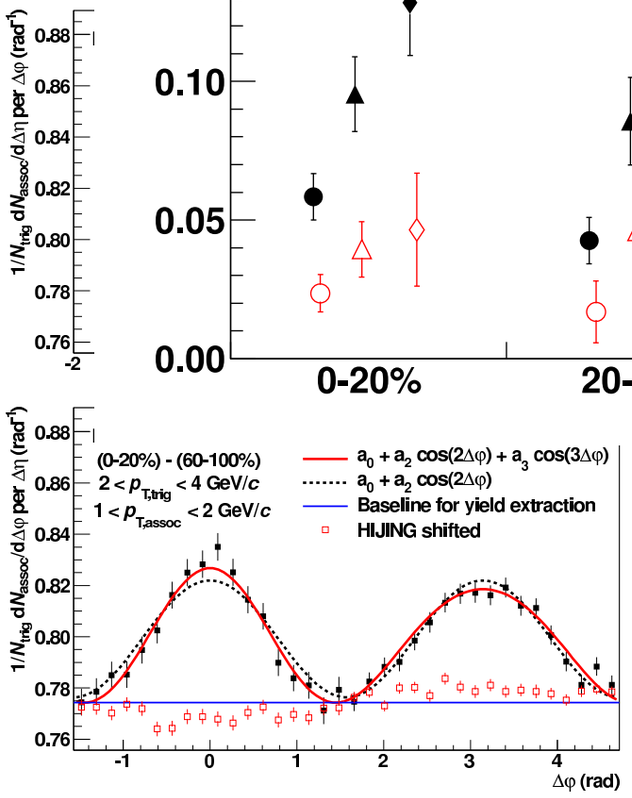

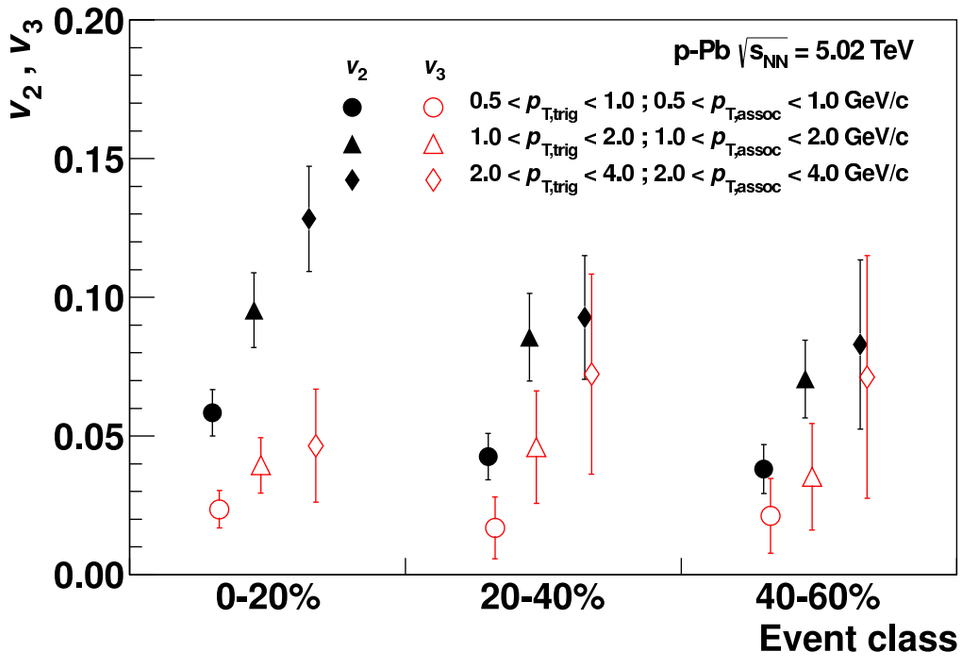

unlike AA, the v2 is dominant v3/v2 = 1/3 or so

all moments grow with pt!

Fig. 3: Left: Associated yield per trigger particle in $\Delta\varphi$ and $\Delta\eta$ for pairs of charged particles with $2 < p_{\mathrm{T,trig}} < 4$ GeV/c and $1 < p_{\mathrm{T,assoc}} < 2$ GeV/c in p–Pb collisions at $\sqrt{s_{\mathrm{NN}}} = 5.02$ TeV for the 0–20% multiplicity class, after subtraction of the associated yield obtained in the 60–100% event class. Top right: the associated per-trigger yield after subtraction (as shown on the left) projected onto $\Delta\eta$ averaged over $|\Delta\varphi| < \pi/3$ (black circles), $|\Delta\varphi - \pi| < \pi/3$ (red squares), and the remaining area (blue triangles, $\Delta\varphi < -\pi/3$, $\pi/3 < \Delta\varphi < 2\pi/3$ and $\Delta\varphi > 4\pi/3$). Bottom right: as above but projected onto $\Delta\varphi$ averaged over $0.8 < |\Delta\eta| < 1.8$ on the near side and $|\Delta\eta| < 1.8$ on the away side. Superimposed are fits containing a $\cos(2\Delta\varphi)$ shape alone (black dashed line) and a combination of $\cos(2\Delta\varphi)$ and $\cos(3\Delta\varphi)$ shapes (red solid line). The blue horizontal line shows the baseline obtained from the latter fit which is used for the yield calculation. Also shown for comparison is the subtracted associated yield when the same procedure is applied on HIJING shifted to the same baseline. The figure shows only statisti-

Observation of Associated Near-side and Away-side Long-range Correlations in $\sqrt{s_{\mathrm{NN}}} = 5.02$ TeV Proton–lead Collisions with the ATLAS Detector

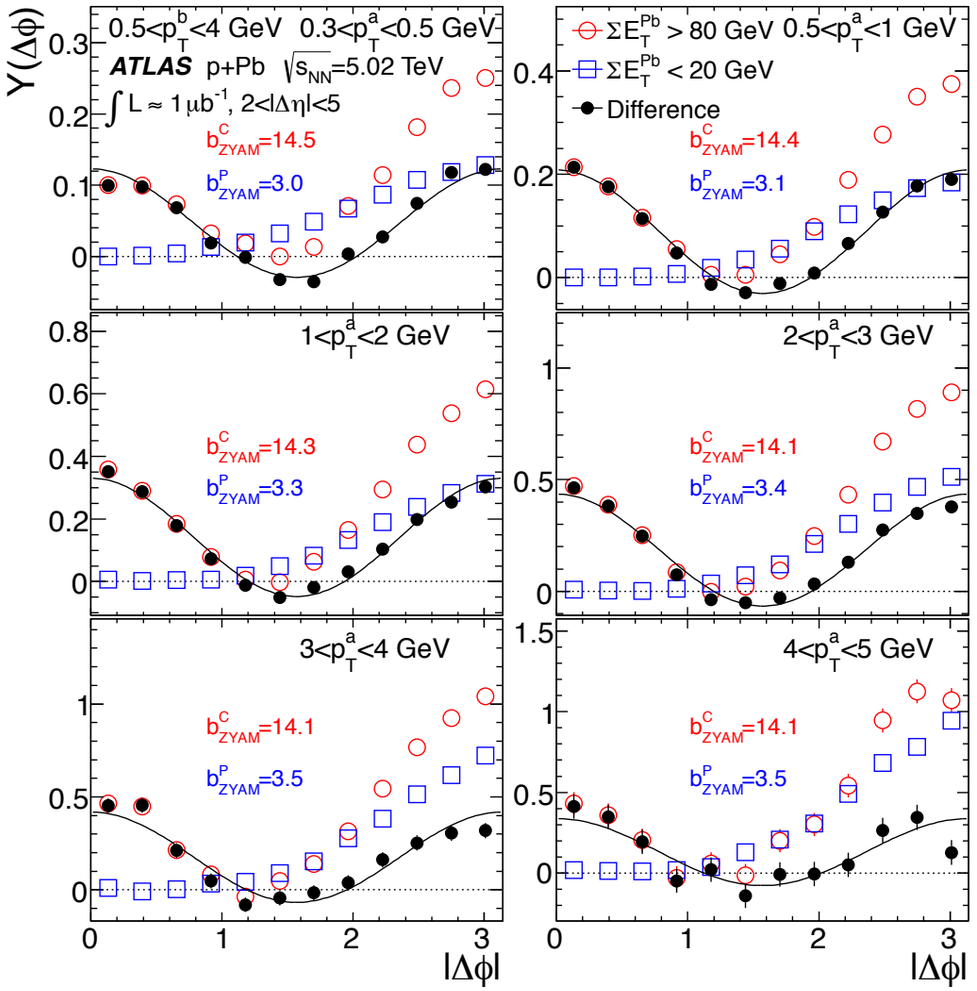

FIG. 3. Distributions of per-trigger yield in the peripheral and the central event activity classes and their differences (solid symbols), for different ranges of $p_{\mathrm{T}}^{\mathrm{a}}$ and $0.5 < p_{\mathrm{T}}^{\mathrm{b}} < 4$ GeV, together with functions $a_0 + 2a_2 \cos 2\Delta\phi$ obtained via a Fourier decomposition (see text). The values for the ZYAM-determined pedestal levels are indicated on each panel for peripheral ($b^{\mathrm{P}}_{\mathrm{ZYAM}}$) and central ($b^{\mathrm{C}}_{\mathrm{ZYAM}}$) $\Sigma E_{\mathrm{T}}^{\mathrm{Pb}}$ bins.

TLAS C

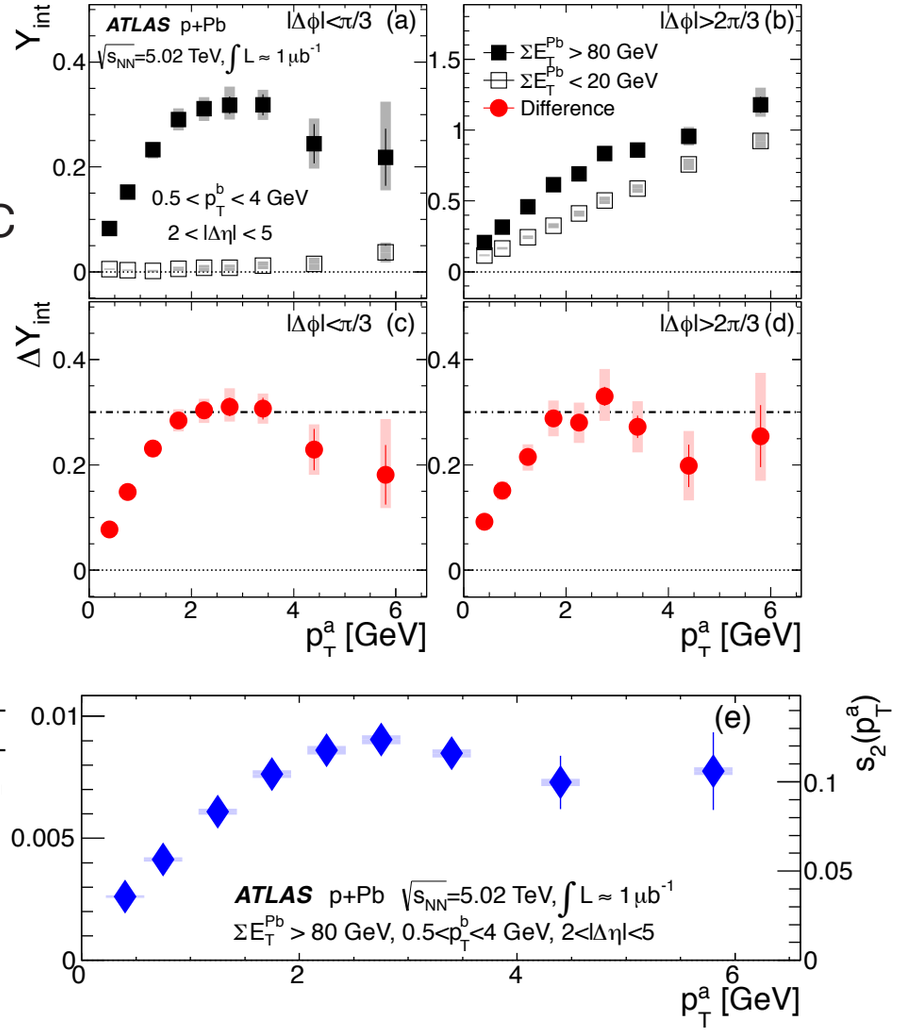

FIG. 4. Integrated per-trigger yields, Y_{int}, (see text) vs $p_{\mathrm{T}}^{\mathrm{a}}$ for $0.5 < p_{\mathrm{T}}^{\mathrm{b}} < 4$ GeV in peripheral and central events, on the (a) near-side and (b) away-side. The panels (c) and (d) show the difference, ΔY_{int}. Panel (e) shows the p_{T} dependence of c_2 (left axis) and s_2 (right axis). The right axis of (e) differs from the left only by a multiplicative factor $1/\sqrt{5.4 \times 10^{-3}}$ (see text). The error bars and shaded boxes represent the statistical and systematic uncertainties, respectively.

Observation of Associated Near-side and Away-side Long-range Correlations in $\sqrt{s_{\mathrm{NN}}} = 5.02$ TeV Proton–lead Collisions with the ATLAS Detector

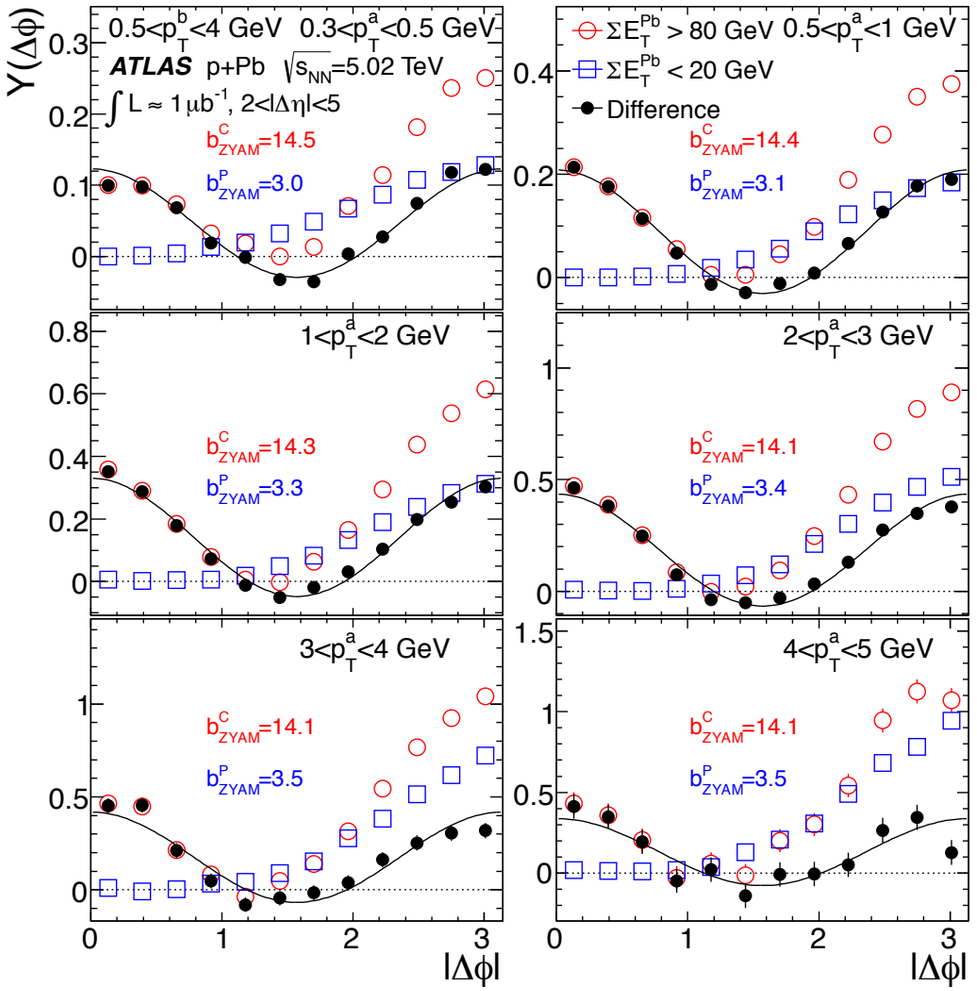

FIG. 3. Distributions of per-trigger yield in the peripheral and the central event activity classes and their differences (solid symbols), for different ranges of $p_{\mathrm{T}}^{\mathrm{a}}$ and $0.5 < p_{\mathrm{T}}^{\mathrm{b}} < 4$ GeV, together with functions $a_0 + 2a_2 \cos 2\Delta\phi$ obtained via a Fourier decomposition (see text). The values for the ZYAM-determined pedestal levels are indicated on each panel for peripheral ($b^{\mathrm{P}}_{\mathrm{ZYAM}}$) and central ($b^{\mathrm{C}}_{\mathrm{ZYAM}}$) $\Sigma E_{\mathrm{T}}^{\mathrm{Pb}}$ bins.

TLAS C

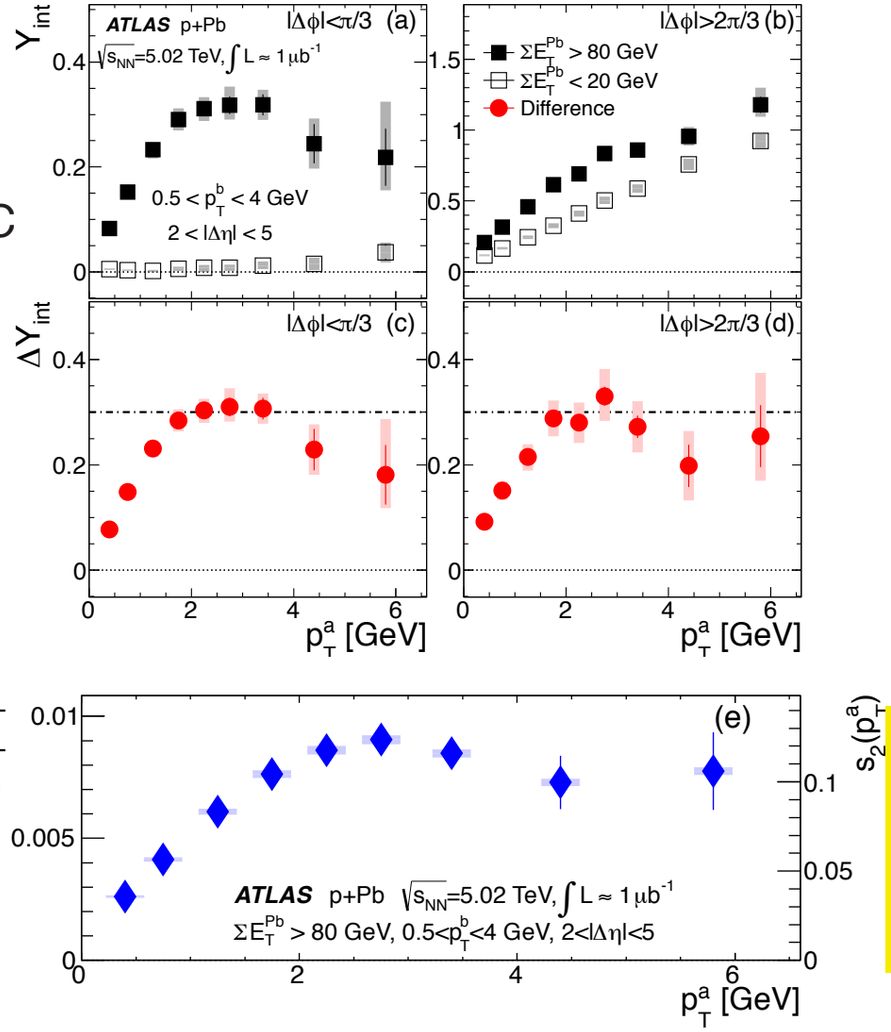

FIG. 4. Integrated per-trigger yields, Y_{int}, (see text) vs $p_{\mathrm{T}}^{\mathrm{a}}$ for $0.5 < p_{\mathrm{T}}^{\mathrm{b}} < 4$ GeV in peripheral and central events, on the (a) near-side and (b) away-side. The panels (c) and (d) show the difference, ΔY_{int}. Panel (e) shows the p_{T} dependence of c_2 (left axis) and s_2 (right axis). The right axis of (e) differs from the left only by a multiplicative factor $1/\sqrt{5.4 \times 10^{-3}}$ (see text). The error bars and shaded boxes represent the statistical and systematic uncertainties, respectively.

persists to high pt

High Multiplicity pp and pA Collisions: Hydrodynamics at its Edge and Stringy Black Hole

Edward Shuryak and Ismail Zahed

- What is the smallest system size which still undergoes a hydrodynamical explosion?

- How do all hydrodynamical observables scale with the system size R and viscosity-to-entropy ratio η/s, for such systems? In particular, how large are the viscous corrections for radial and elliptic flows?

- How do amplitudes of higher angular harmonics v_n scale with n,R and η/s? In which p_t region do we expect hydrodynamics to work, and for each v_n?

- Do high multiplicity pp and pA collisions in which the (double) "ridge" has been recently observed at LHC [7–9] fit into such a hydrodynamical scaling?

two small parameters of hydro

$$\mathcal{O}(1) \approx \frac{1}{TR^{pp,high\ mutiplicity}} \qquad (2)$$
$$> \frac{1}{TR^{central\ pA}} > \frac{1}{TR^{central\ AA}} \approx \mathcal{O}(1/10)$$

Another important small parameter which we seem to have for strongly coupled Quark-Gluon Plasma (sQGP) is the *viscosity-to-entropy-density ratio*

$$\frac{\eta}{s} \approx \mathcal{O}(1/10) \ll 1 \qquad (3)$$

Roughly speaking, it tells us that viscous effects – or the mean free path – is additionally suppressed compared to the micro scale $1/T$.

the radial (Gubser's) flow

$$v_\perp^{max}[AA, pA, pp] = [0.69, 0.83, 0.95]$$

Gubser's solution of ideal relativistic hydrodynamics, for the transverse velocity and the energy density reads

$$v_\perp(t,r) = \frac{2tr}{1+t^2+r^2} \qquad (10)$$

$$\frac{\epsilon}{q^4} = \frac{\hat{\epsilon}_0 2^{8/3}}{t^{4/3}\left[1+2(t^2+r^2)+(t^2-r^2)^2\right]^{4/3}}$$

$$t = q\bar{\tau}, \quad r = q\bar{r}$$

$$q_{AA}^{-1} = 4.3, \; q_{pA}^{-1} = 1, \; q_{pp}^{-1} = 0.5\,(fm)$$

my guesses of the
system's size
central PbPb 400
pA: 15-20 participants
pp 2

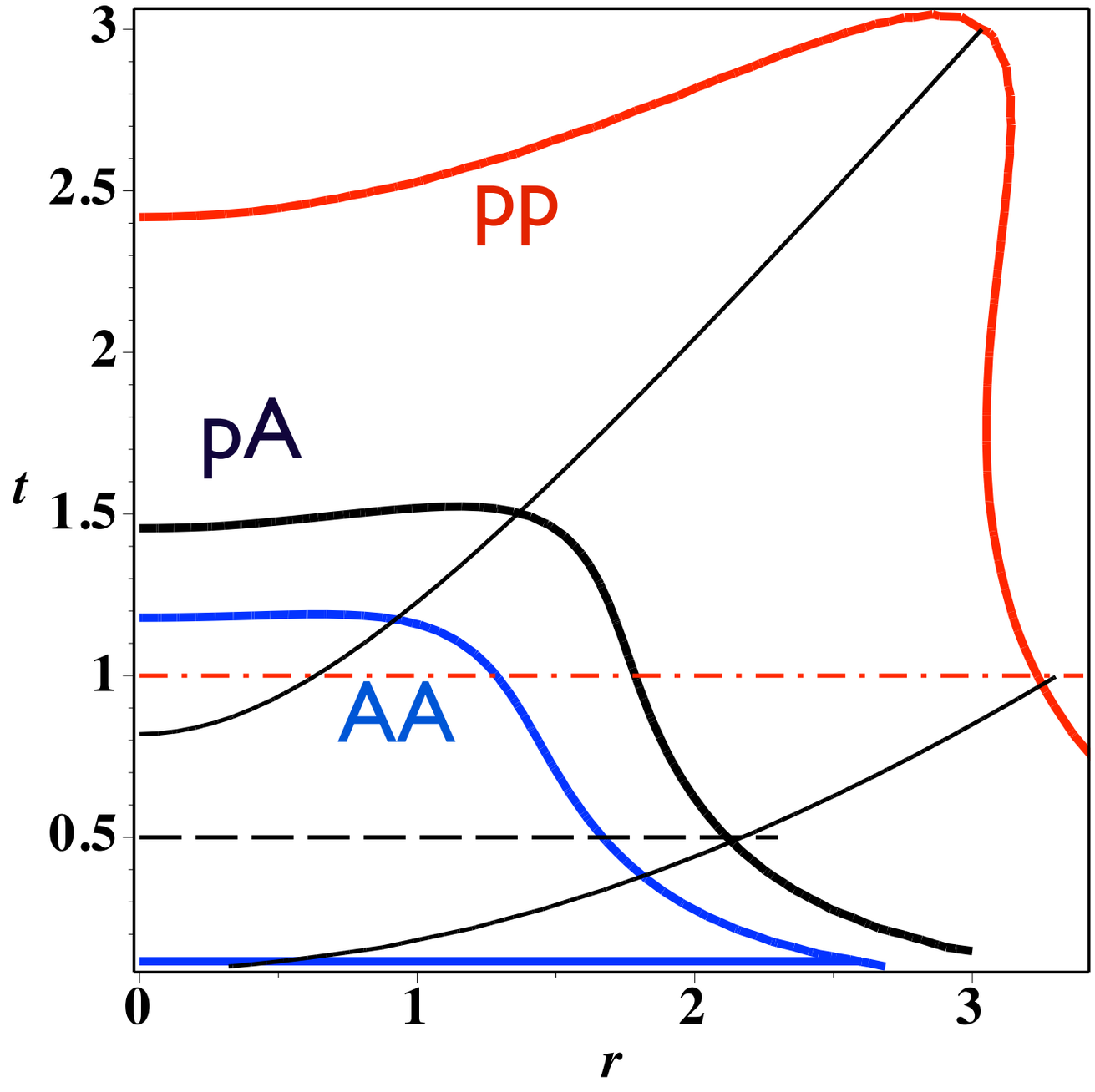

the role of viscosity

$$H_0 = \frac{\eta}{\epsilon^{3/4}} = \frac{\eta}{s}\frac{4}{3} f_*^{1/4} \qquad (20)$$

for $\eta/s = 0.134$ we will use as representative number $H_0 = 0.33$.

nonzero viscosity the solution is

$$\hat{T} = \frac{\hat{T}_0}{(\cosh\rho)^{2/3}} + \frac{H_0 \sinh^3\rho}{9(\cosh\rho)^{2/3}} \times {}_2F_1\left(\frac{3}{2}, \frac{7}{6}; \frac{5}{2}, -\sinh^2\rho\right) \qquad (27)$$

with $\hat{T} = \tau f_*^{1/4} T$ and $f_* = \epsilon/T^4 = 11$ as in [18].

In [19] Gubser and Yarom re-derived the radial solution by going into the co-moving frame via a coordinate transformation from the τ, r to a new set ρ, θ given by:

$$\sinh\rho = -\frac{1-\tau^2+r^2}{2\tau} \qquad (25)$$

$$\tan\theta = \frac{2r}{1+\tau^2-r^2} \qquad (26)$$

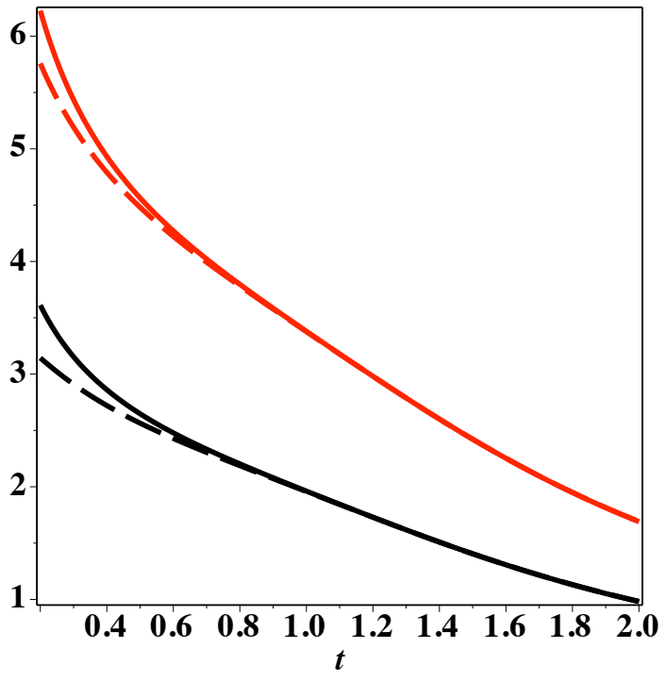

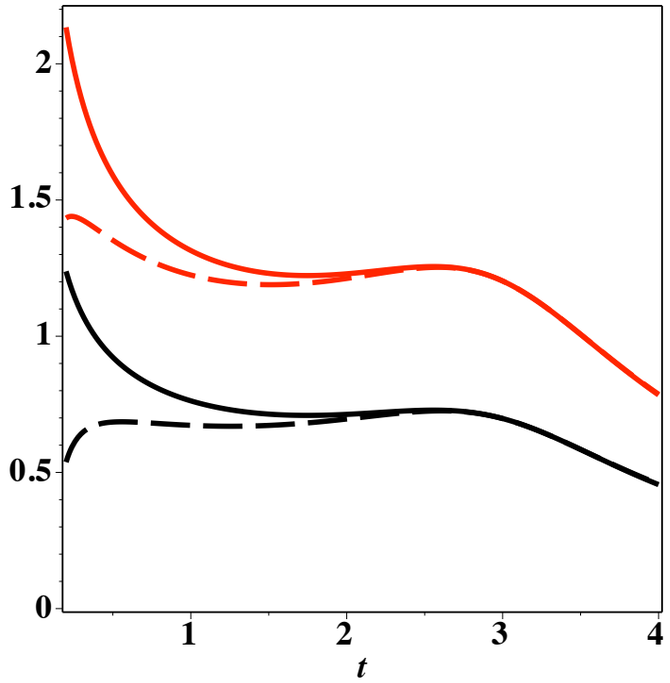

The radial flow in pA,pp has moderate corrections!

FIG. 3: (color online) The temperature versus dimensionless time t, for ideal hydrodynamics (solid) and viscous hydrodynamics with $\eta/s = 0.132$ (dashed) lines. The upper pair of (red) curves are for pp, the lower (black) ones for pA collisions. The upper plot is for $r = 1$, the lower plot for $r = 3$.

viscosity for higher harmonics

Staig+ES (2010) suggested to use ``acoustic'' damping expression

t=O(R)

$$P_m = \exp\left[-m^2 \frac{4}{3}\left(\frac{\eta}{s}\right)\left(\frac{1}{TR}\right)\right]$$

AA

pA

pp

viscosity for higher harmonics

Staig+ES (2010) suggested to use ``acoustic'' damping expression

t=O(R)

$$P_m = \exp\left[-m^2 \frac{4}{3}\left(\frac{\eta}{s}\right)\left(\frac{1}{TR}\right)\right]$$

In AA: (m/10)^2
in pA/pp (m/3)^2

AA

pA

pp

viscosity for higher harmonics

Staig+ES (2010) suggested to use ``acoustic" damping expression

t=O(R)

$$P_m = \exp\left[-m^2 \frac{4}{3}\left(\frac{\eta}{s}\right)\left(\frac{1}{TR}\right)\right]$$

In AA: (m/10)^2
in pA/pp (m/3)^2

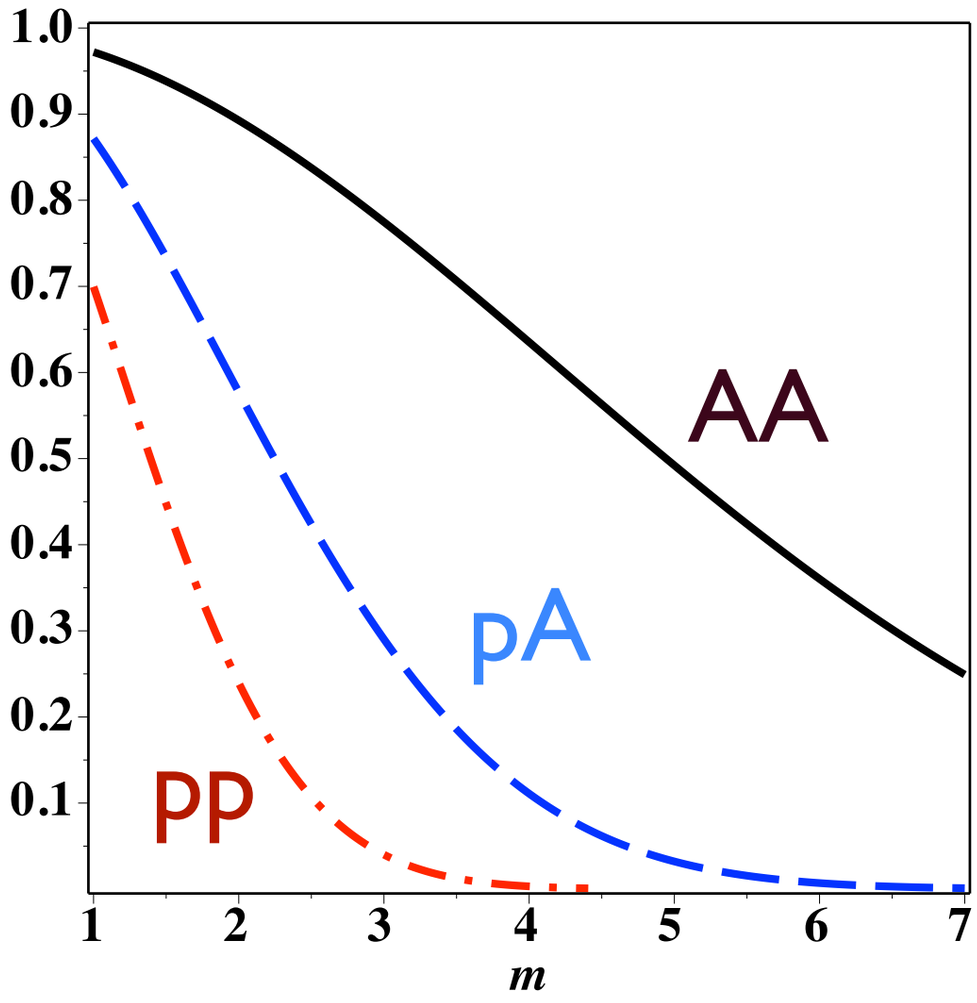

FIG. 4: (color online) Squared amplitude dissipation factor P_m^2 (as it appears in 2-particle correlators) for $\eta/s = .134$ as a function of the azimuthal harmonics m for AA (black) solid, pA (blue) dash and pp (red) dash-dot.

Is anisotropic flow really acoustic?

Roy A. Lacey,[1,*] Yi Gu,[1] X. Gong,[1] D. Reynolds,[1] N. N. Ajitanand,[1] J. M. Alexander,[1] A. Mawi,[1] and A. Taranenko[1]

[1] *Department of Chemistry, Stony Brook University, Stony Brook, NY, 11794-3400, USA*

(Dated: January 3, 2013)

$$P_m = \exp\left[-m^2 \frac{4}{3}\left(\frac{\eta}{s}\right)\left(\frac{1}{TR}\right)\right]$$

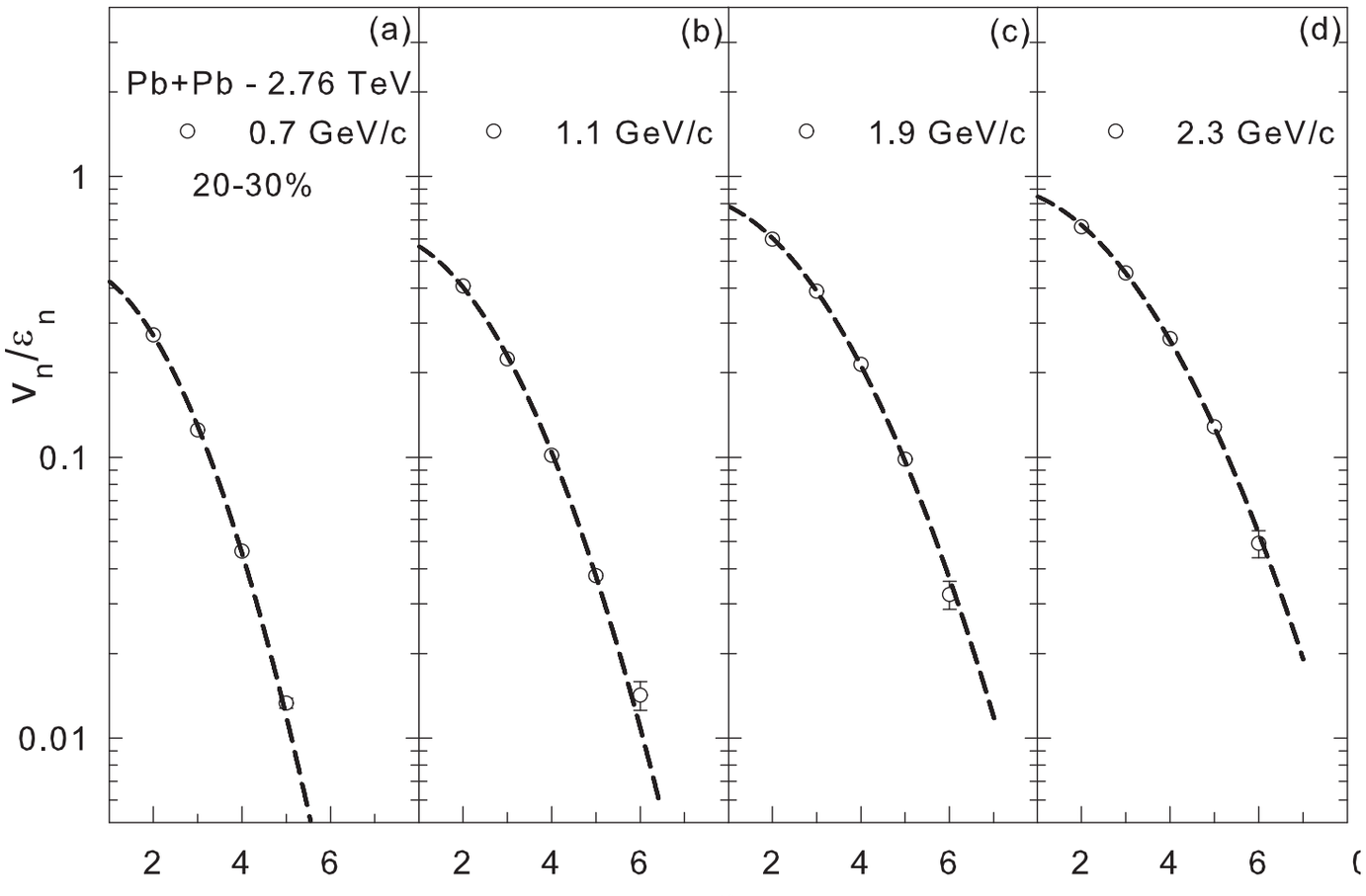

Harmonics 2,3,4 for AA,pA,pp

stronger damping in pA,pp

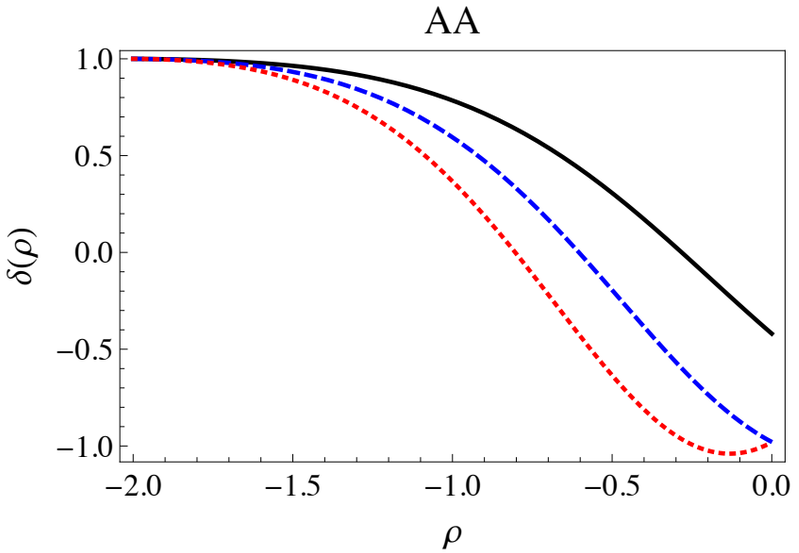

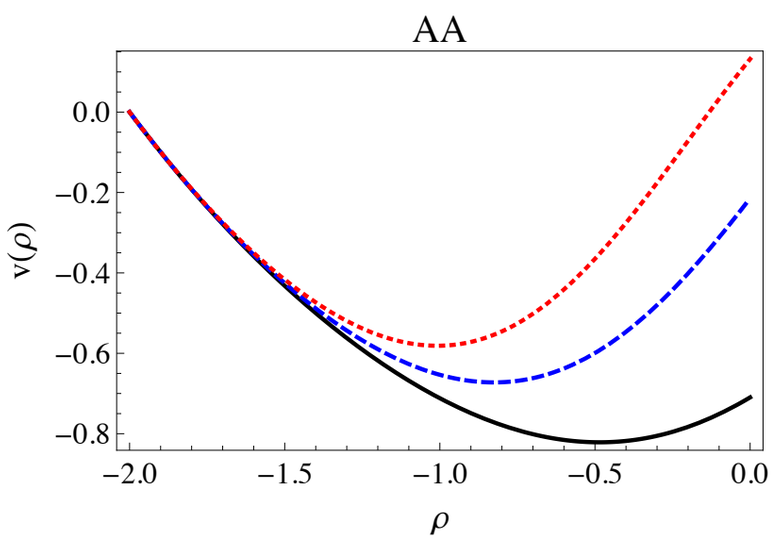

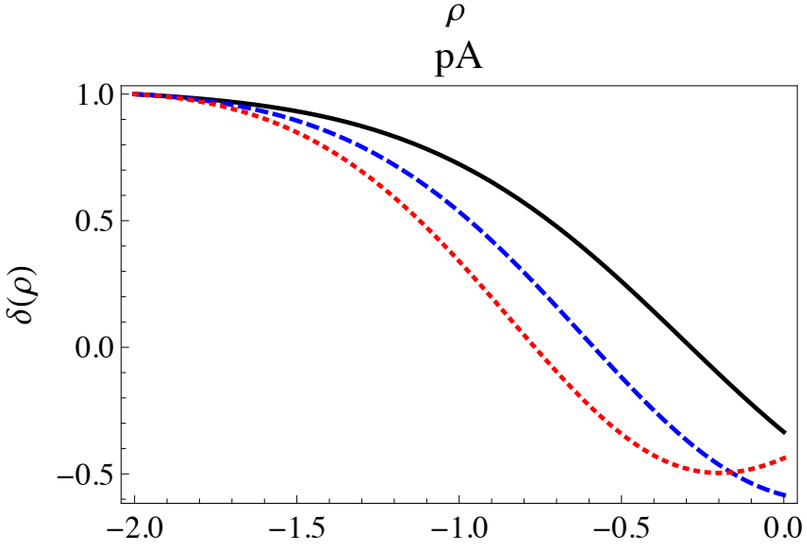

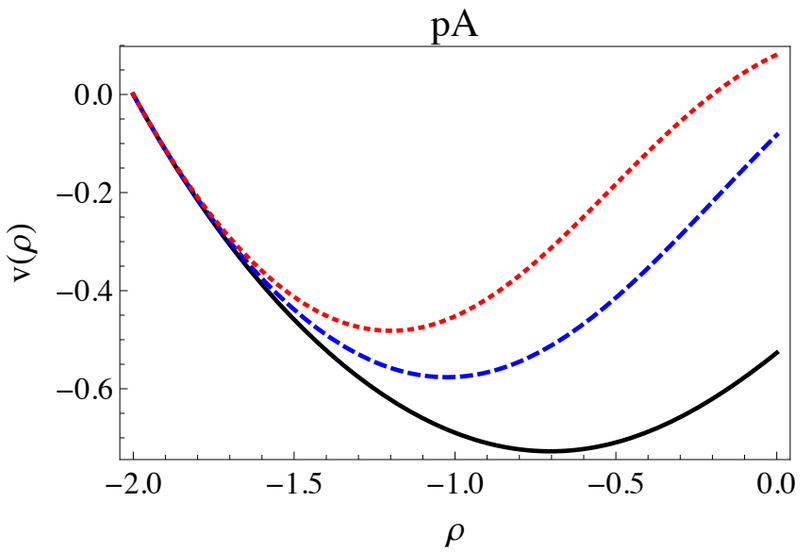

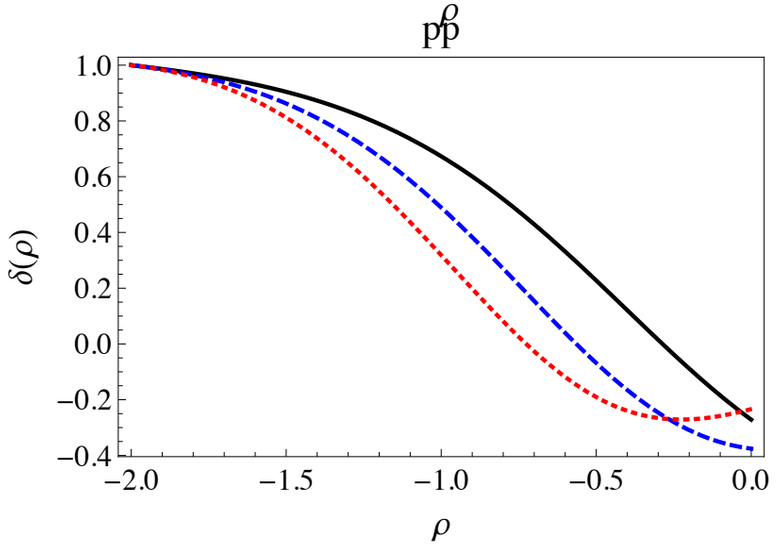

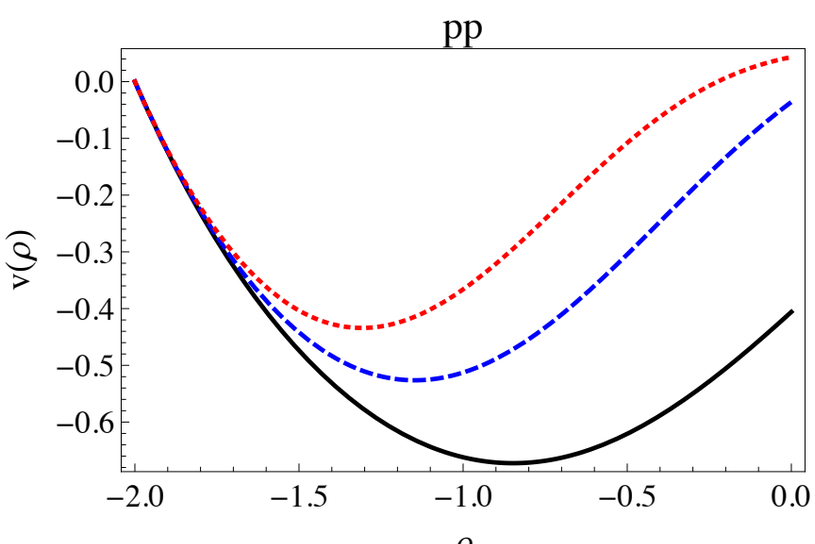

$$(v_2^{AA})^2 : (v_2^{pA})^2 : (v_2^{pp})^2 = 0.5(\epsilon_2^{AA})^2 : 0.3(\epsilon_2^{pA})^2 : 0.16(\epsilon_2^{pp})^2 \quad (36)$$

This is qualitatively consistent with the *squared* damping of the amplitude of the previous section, for $m = 2$.

A comparison to CMS data shows that the pp data show smaller v_2 as compared to pA data. Quantitatively, the ratio is about factor 1/4 (see Fig.3 of [7]) rather than 1/2 which the hydro solution provides. Perhaps it is because the pp collisions create a somewhat more spherical fireball, with $\epsilon_2^{pp} < \epsilon_2^{pA}$, in spite of being smaller in size. We will return to this issue at the end of the paper.

small v3/v2

ratio of the $m = 3$ to $m = 2$ harmonics

$$\left(\frac{v_3^{AA}}{v_2^{AA}}\right)^2 \approx 0.12 \left(\frac{\epsilon_3^{AA}}{\epsilon_2^{AA}}\right)^2 \quad (37)$$

$$\left(\frac{v_3^{pA}}{v_2^{pA}}\right)^2 \approx 0.09 \left(\frac{\epsilon_3^{pA}}{\epsilon_2^{pA}}\right)^2$$

$$\left(\frac{v_3^{pp}}{v_2^{pp}}\right)^2 \approx 0.02 \left(\frac{\epsilon_3^{pp}}{\epsilon_2^{pp}}\right)^2$$

Assuming $\epsilon_3/\epsilon_2 \sim 1$ one finds that in pA we predict $v_3/v_2 \approx 1/3$, which agrees nicely with the ALICE data [8]. For pp we have $v_3/v_2 \approx 1/7$ which is probably too small to be seen.

resummation of higher gradients a la Lublinsky-Shuryak

An approximate PADE-like re-summation of the higher order terms has been suggested by Lublinsky and Shuryak (LS) [20]. The main point is to notice the alternating signs of the series, which calls for an resummation a la geometrical series. Here we discuss only the single pole resummation model or LS2 in [20] in which the Navier-Stokes viscosity or NS is subtituted by an effective viscosity

$$\eta_{LS2}(\omega,k)=\frac{\eta_{NS}}{1-\eta_{2,0}k^2/(2\pi T)^2-i\omega\eta_{0,1}/(2\pi T)} \tag{40}$$

Note that (40) involves only two dimensionless coefficients

$$\eta_{2,0}=-\frac{1}{2}\ \eta_{0,1}=2-\ln 2=1.30 \tag{41}$$

Schematically the resummed hydro equations look as

$$(Euler)=\eta\mathbf{O}_{LS}(Navier-Stokes) \tag{44}$$

where $\mathbf{O}_{LS}$ is an integral operator. However, one can act with its inverse on the hydrodynamical equation as a whole, acting on the Euler part but canceling it in the viscous term

$$\mathbf{O}_{LS}^{-1}(Euler)=\eta(Navier-Stokes) \tag{45}$$

These are the equations of the LS hydrodynamics. Obviously they have two extra derivatives and thus need more initial conditions for solution.

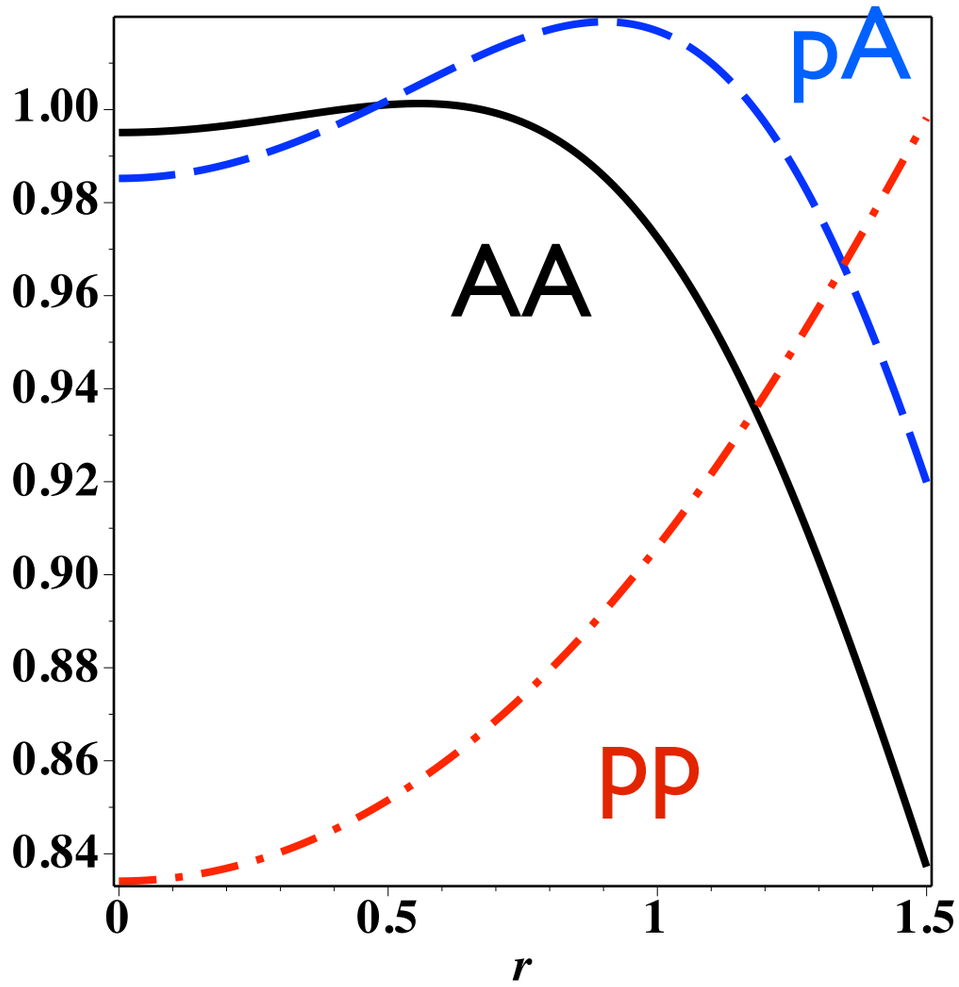

$$\mathbf{O}_{LS}^{-1}(f)=\quad 1+\frac{q^2}{2(2\pi T)^2}\left(\frac{\partial^2 f}{\partial r^2}+\frac{1}{r}\frac{\partial f}{\partial r}\right)\frac{1}{f}$$
$$+\ (2-\ln 2)\,\frac{q}{2\pi T}\frac{\partial f}{\partial t}\frac{1}{f} \tag{43}$$

summary of the hydro

- the applicability of hydrodynamics rests on two small parameters:
  (i) **the micro-to- macro ratio 1/TR, (ii) the viscosity-to-entropy ratio η/s.**
  For central AA collisions, both are O(1/10). For high multiplicity pA and pp collisions, the first parameter is no longer small 1/TR = O(1), prompting us to ask which hydrodynamical predictions are preserved by the smallness of only the second parameter η/s.

- After solving the hydrodynamical equations we found that **the radial (axially symmetric) flow is little modified by viscosity and is in fact enhanced** by higher transverse gradients. Thus our main prediction is an enhanced radial flow => a change in the observed pt spectra on the particle mass, or growing proton-to-pion-ratio with pt. The magnitude of the effect should be even larger **(=> ALICE ?)**

- **Higher harmonics are penalized by larger viscous corrections**. We obtained explicit solution for Gubser flow for m = 2, 3, 4 as shown in Fig.5. We have found a small v3/v2 ≈ 1/3 ratio for pA in agreement with the reported ALICE data (in contrast to v3/v2 >1 in central AA). The value of v2 itself is also suppressed by viscosity, and the relative suppression we have found between the pp and pA collisions agree reasonably with the CMS data.

Staig+ES 2011
prediction vs ATLAS data